Application of a Differential Fuel-Cell Analyzer for Measuring Atmospheric Oxygen Variations

BRITTON B. STEPHENS

Earth Observing Laboratory, National Center for Atmospheric Research, Boulder, Colorado*

PETER S. BAKWIN AND PIETER P. TANS

NOAA/Climate Monitoring and Diagnostics Laboratory, Boulder, Colorado

RON M. TECLAW AND DANIEL D. BAUMANN

Forest Sciences Laboratory, USDA Forest Service, Rhinelander, Wisconsin

(Manuscript received 19 December 2005, in final form 10 May 2006)

ABSTRACT

A commercially available differential fuel-cell analyzer has been adapted to make field-based ppm-level measurements of atmospheric O_2 variations. With the implementation of rapid calibrations and active pressure and flow control, the analysis system described here has a 1σ precision of ± 2.5 per meg (≈ 0.5 ppm) for a 2-min measurement. Allowing for system stabilization after switching inlet lines, a 6-min measurement with a precision of ± 1.4 per meg (≈ 0.3 ppm) every 20 min is obtained. The elimination of biases in any atmospheric O_2 measurement depends critically on careful gas-handling procedures, and after screening for known sources of bias a comparability of ± 10 per meg (≈ 2 ppm) with the present setup is estimated. In comparison to existing techniques, the relatively small size, low cost, fast response, motion insensitivity, and ease of implementation of the fuel-cell analyzer make it particularly useful for a wide range of unattended field applications. This system has been used to measure atmospheric O_2 concentrations at the WLEF tall-tower research site in northern Wisconsin semicontinuously from June 2000 to December 2003. These measurements represent the first extended O_2 record in and above a forest ecosystem, and are being used to investigate global carbon budgeting, plant physiology, continental boundary layer mixing and synoptic transport, and potential means of industrial emission verification. In this paper, the measurement technique is described in detail and several weeks of data are presented to illustrate its performance.

1. Introduction

Marine boundary layer atmospheric O_2 measurements have proven to be valuable constraints on the global partitioning of terrestrial and oceanic CO_2 sources, seasonal net production by the marine biosphere, hemispheric gas exchange rates, and interhemispheric oceanic transport (Keeling and Shertz 1992; Bender et al. 1996; Keeling et al. 1996, 1998b; Stephens et al. 1998; Battle et al. 2000; Manning and Keeling 2005). The precision requirements for these measurements are challenging, with background variations of interest on the order of 1–100 per meg (Keeling et al. 1993), where

$$\delta(O_2/N_2)\ (\text{per meg}) = \left[\frac{(O_2/N_2)_{\text{sample}}}{(O_2/N_2)_{\text{reference}}} - 1\right] \times 10^6. \quad (1)$$

In this context, the addition of 1 μmol of O_2 to 1 mol of dry air results in a change of 4.8 per meg (Keeling et al. 1998a). Existing techniques for measuring parts per million (ppm)-level background O_2 variations now include interferometric (Keeling 1988), mass spectro-

* The National Center for Atmospheric Research is sponsored by the National Science Foundation.

Corresponding author address: Dr. Britton Stephens, National Center for Atmospheric Research, Earth Observing Laboratory, 1850 Table Mesa Dr., Boulder, CO 80305.
E-mail: stephens@ucar.edu

DOI: 10.1175/JTECH1959.1

metric (Bender et al. 1994), paramagnetic (Manning et al. 1999), vacuum ultraviolet absorption (Stephens 1999; Stephens et al. 2003), and gas chromatography (Tohjima 2000). However, for autonomous in situ measurements, these methods all have specific disadvantages; the instruments are either too large, too expensive, or too motion sensitive, or require either extensive construction, frequent user intervention, or too much time to obtain a precise measurement. We present here a new technique, based on a commercially available differential fuel-cell analyzer, that addresses these limitations and significantly advances our atmospheric O_2 measurement capabilities.

The advanced capabilities of the fuel-cell analyzer can enable a wide range of new studies. For example, the fuel-cell O_2 measurement system can be used to improve the temporal resolution of marine boundary layer records typically based on flask sampling, thereby significantly advancing our understanding of seasonal marine productivity and episodic oceanic O_2 fluxes (Manning et al. 1999; Lueker et al. 2003). In addition, this system can be used to improve upon the spatial and temporal resolution of shipboard flask measurements, which will help to address uncertainties in meridional atmospheric O_2 gradients and their implications for large-scale ocean circulation (Stephens 1999; Stephens et al. 2003; Thompson 2005; Tohjima et al. 2005; Battle et al. 2006). The development of this robust in situ technique has also allowed us to extend atmospheric O_2 measurements from the marine boundary layer to the interior of continents, and to apply these continental measurements to study global CO_2 budgeting, terrestrial biospheric processes, atmospheric transport, and industrial emissions.

Presently, observed trends in atmospheric O_2 provide our best constraint on the long-term global partitioning of terrestrial and oceanic sinks for anthropogenic CO_2 (Houghton et al. 2001). A key value in calculating this partitioning is the assumed O_2:CO_2 ratio for the terrestrial uptake of anthropogenic CO_2. The relationship between O_2 and CO_2 during terrestrial exchange is not exactly 1 because of the incorporation of nitrogen and other species during photosynthesis, and their oxidation during respiration. Keeling (1988) estimated an oxidation ratio ($OR = -O_2{:}CO_2$) for wood of 1.05 based on a survey of elemental abundance studies. Severinghaus (1995) measured oxidation ratios of around 1.2 for forest soil samples, but estimated that the net ecosystem exchange occurs at a ratio closer to 1.1. The OR for respiration in forest soils and roots depends on the form of nitrogen (NO_3^- or NH_4^+) produced by soil microbes and utilized by trees (Bloom et al. 1989, 1992). However, this fundamental distinction is not widely characterized in nature and is ignored in most terrestrial ecosystem models. Furthermore, the photosynthetic quotient ($PQ = O_2{:}-CO_2$) for trees also depends on the allocation of new carbon to either wood or nitrogen-rich leaves and fine roots. The ability to measure this partitioning would be very useful in identifying the growth stage of a forest and locating net carbon sinks. Existing flask-based studies of terrestrial O_2:CO_2 ratios are limited by the number and scatter of the available data points (Seibt et al. 2004; Marca 2004; Sturm et al. 2005a). Thus, continuous measurements of atmospheric O_2 and CO_2 in a forest environment can improve our constraints on the terrestrial O_2:CO_2 value used to partition global CO_2 sinks, and they can have direct impacts on our understanding of the physiological behavior of forest plants.

By combining O_2 and concurrent CO_2 measurements, we can derive the tracer atmospheric potential oxygen ($APO \approx O_2 + 1.1\ CO_2$; Stephens et al. 1998). The definition of APO includes the simplifying assumption of a constant and known O_2:CO_2 ratio, but to the extent that photosynthesis and respiration do not change this scaled sum of O_2 and CO_2, APO is conservative with respect to terrestrial processes. In contrast, because air–sea O_2 and CO_2 fluxes are largely decoupled, APO provides a sensitive tracer for oceanic gas exchange. Continental interior observations of this primarily oceanic tracer can then provide valuable information on aspects of continental boundary layer mixing and synoptic-scale transport that can be used to validate atmospheric models. For example, measurements of the APO gradient between the North Pacific and the central United States can help to constrain the seasonal variation in continental boundary layer mixing, which is a dominant source of uncertainty in global CO_2 inversions (Denning et al. 1995; Gurney et al. 2002).

The O_2:CO_2 ratios for fossil fuel combustion vary from −1.95 for natural gas, to −1.44 for liquid fuels, to −1.17 for coal (Keeling 1988). Because of this, atmospheric O_2 measurements can help to distinguish between industrial and terrestrial influences on observed CO_2 variations. Furthermore, it may be possible to use atmospheric O_2 measurements in future international emission verification efforts. For example, if we knew how much natural gas and liquid fuel were being combusted in a particular country, we could measure the O_2:CO_2 ratio in downwind pollution signals to estimate how much coal was also being burned. We can test this idea by measuring O_2:CO_2 ratios in continental U.S. pollution events and comparing them to those expected from reported distributions of fuel types for the source regions.

To investigate these various processes and applications, in June of 2000 we installed the differential fuel-cell analyzer and associated equipment described here for ongoing O_2 measurements at the WLEF tall-tower research site (Bakwin et al. 1998; Davis et al. 2003) in northern Wisconsin. More recently, similar systems have been installed at a tall-tower site in Ochsenkopf, Germany (A. Manning 2003, personal communication), on research ships in the Southern Ocean (Thompson 2005), and at Harvard Forest, Massachusetts (M. Battle 2005, personal communication); and installation has been planned at Mace Head, Ireland (R. Keeling, 2005 personal communication) and Syowa, Antarctica (T. Nakazawa 2005, personal communication). To assist in this growing use of fuel-cell O_2 analyzers, we provide a detailed description of our WLEF implementation in section 2. Also, as expected with the exploratory nature of this project, we have encountered a number of unique challenges to making accurate continuous O_2 measurements, and we share what we have learned about potential sources of measurement bias associated with fractionation in reference cylinders, at tubing tee junctions, and at sample inlets. We will present the major results from the first three-and-a-half years of measurements in a subsequent publication, but present several weeks of data here in section 3 to demonstrate the performance and potential applications of this measurement approach.

2. Instrument description and performance

Figure 1 shows a schematic of the instrumentation and gas-handling hardware we have implemented at the WLEF tall-tower site for background atmospheric O_2 measurements.

a. O_2 analyzer

The Sable Systems Oxzilla I differential O_2 analyzer is based on a comparison of potentials from two lead–oxygen fuel cells. These cells contain a weak acid electrolyte, which is isolated from air by a gas-permeable membrane, and within which the net reaction

$$O_2 + 4H^+ + 2Pb \rightarrow 2H_2O + 2Pb^{++} \qquad (2)$$

takes place. The voltage across the cell is thus proportional to the rate at which O_2 diffuses across the membrane, which in turn is proportional to the partial pressure of O_2 in the analyzed airstreams. By differencing the voltages from the two cells, most sources of drift in the signals can be eliminated, and a very precise measurement is produced. For differential measurements, the Oxzilla I came with a quoted short-term noise of 2 ppm (≈10 per meg) and a long-term drift of 20 ppm (≈100 per meg). For our unit we found a differential 1σ precision at the serial data output rate of 1.16 Hz of 25 per meg, and drift rates in the differential signal of 100 per meg over several hours. The analyzer also does not appear to be adversely affected by acceleration or vibration.

To improve the instrument for background atmospheric O_2 measurements we made several modest changes to the off-the-shelf unit. Because differential permeation of O_2 and N_2 through plastic tubing can have significant effects on O_2 mole fractions, we removed the internal plastic tubing and filters and replaced them with 2-mm inner-diameter (ID) stainless steel tubing. Also, because gas temperatures equilibrate very rapidly in metal tubing, we removed the original heat exchanger tubing coil and fan. To avoid the potential for small downstream pressure differences, we plumbed the two sample-cell outlets and the internal pressure sensor into a common volume immediately downstream of the cells. Finally, to minimize absolute and differential pressure fluctuations in the air flowing past the fuel cells, we actively control mass flow and pressure at various points, as shown in Fig. 1.

To improve upon the precision and stability characteristics, we rapidly switch sample and reference gases between the two cells, using an upstream four-way valve (see Fig. 1) composed of two miniature solenoid valves and a manifold (Numatics, TM series). The diffusivity of the fuel-cell membranes leads to a characteristic response time for the sensors of 12 s to reach 90% of a step change. Therefore, we switch every 64.5 s (75 serial data values) and ignore the first 21.5 s (25 serial data values) of data after each switch. An example of the resulting signal when switching between two known calibration gases is shown in Fig. 2. Because the Oxzilla differential signal represents alternately gas A − gas B and then gas B − gas A, the measured amplitude of this square wave ($\Delta_{1\text{-min}}$) represents 2 × gas A − 2 × gas B. By switching in this manner we eliminate most sources of drift with time scales longer than 1 min, and we increase the sensitivity of the measurement by a factor of 2. The 1σ precision on an average of the differential signal over one 43-s period is 3.5 per meg, which is consistent with a standard error from averaging 50 values having white noise of 25 per meg. The precision on $\Delta_{1\text{-min}}$ is 2.5 per meg in the actual concentration difference between the two switched gases, which is consistent with summing two 3.5 per meg errors in quadrature then dividing by a factor of 2. The drift rate on $\Delta_{1\text{-min}}$ is typically 2.5 per meg over 6 h, which ultimately determines the required calibration frequency.

To convert the Oxzilla measurements of apparent

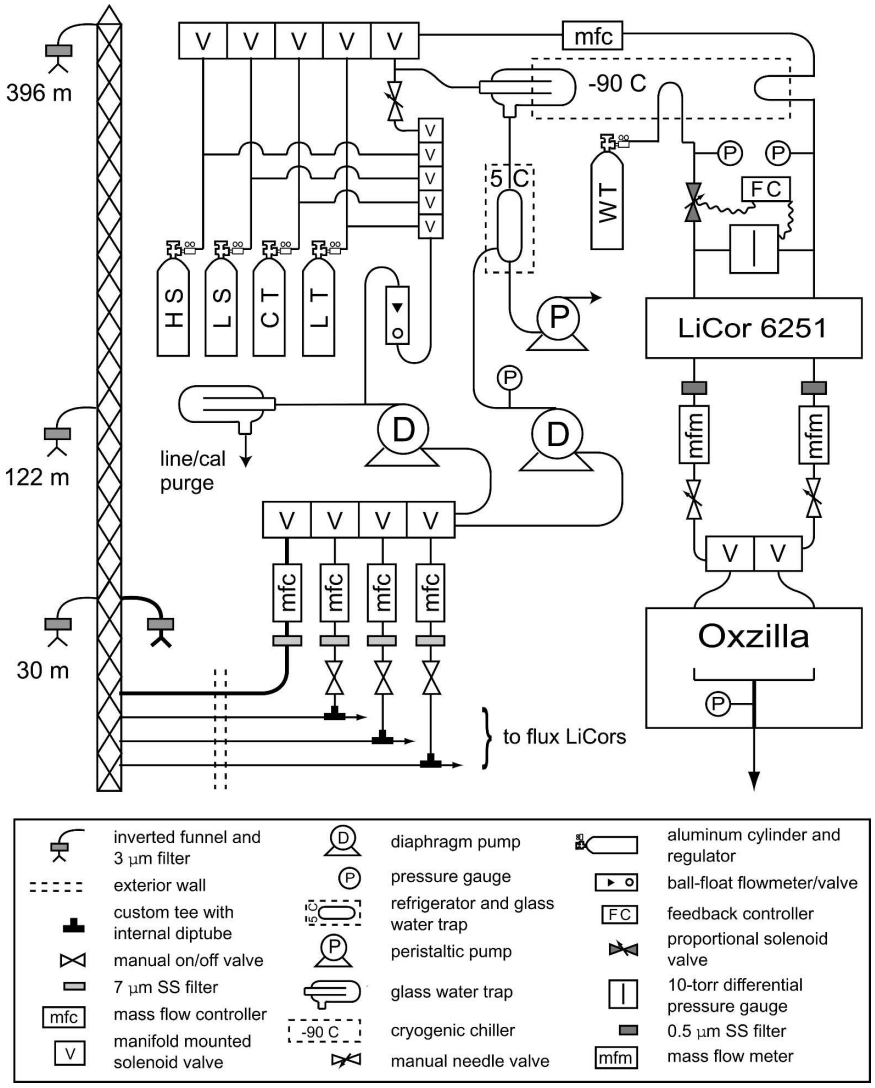

FIG. 1. Schematic and legend showing the gas-handling arrangement as implemented at the WLEF tall tower. Components are included for air sampling, air drying, calibration, regulator and sample line purging, active flow and pressure control, and O_2 and CO_2 analysis.

mole fraction into relative per-meg units requires correcting for the diluting effect of changing CO_2 concentrations (Keeling et al. 1998a). We first convert our reference gas $\delta(O_2/N_2)$ values into apparent mole fraction differences (δX_{O_2}) using their known CO_2 concentrations. Then, after linearly interpolating the Oxzilla differential signals to get apparent sample mole fraction differences we convert these values back into relative per-meg units using simultaneously measured CO_2 concentrations. All of these conversions are captured in the following equation [from Keeling et al. 1998a, their Eq. (4)]:

$$\delta(O_2/N_2) = \frac{\delta X_{O_2} + X_{O_2}([CO_2] - 363.29)}{X_{O_2}(1 - X_{O_2})}, \quad (3)$$

where the O_2 mole fraction (X_{O_2}) is 0.2095, $[CO_2]$ is the measured CO_2 concentration (μmol mol^{-1}) in dry air for the sample gas, and 363.29 is the average CO_2 concentration of the reference cylinders defining zero on the Scripps O_2 scale. This conversion assumes that N_2 and Ar are constant, so it is important to only apply it in situations where the references gases are composed of natural air.

In addition to the modifications just described, a number of other conditions must be met to make comparable background atmospheric O_2 measurements. These include 1) using reference gases tied to established calibration scales and introducing them to the instrument at the appropriate frequency, pressure, and flow; 2) providing suitable flows through sample inlet

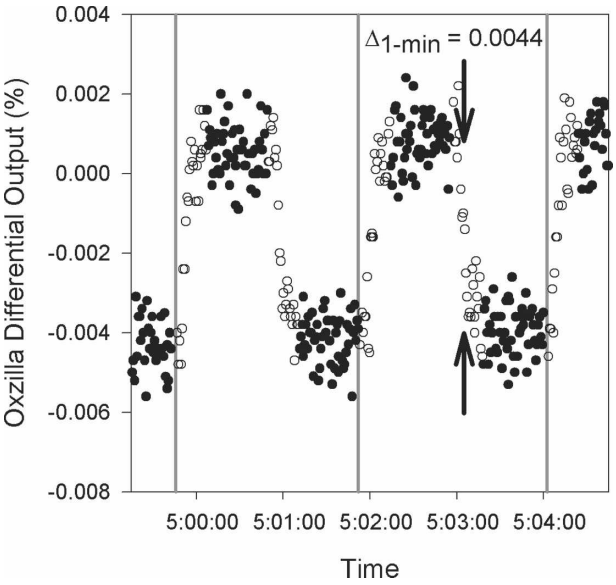

FIG. 2. Example of the Oxzilla differential O_2 signal over several 1-min switching cycles, while comparing two reference gases. The vertical gray lines indicate the time at which the changeover valve is switched and open circles show data that are ignored after each switch. In this case the gases have an apparent O_2 mole fraction difference of 0.0022%, which results in a signal amplitude of 0.0044% because of the crossover switching arrangement.

lines and the instrument while avoiding fractionation effects at inlets and tubing junctions; 3) drying the sample and calibration gases to below several ppm of H_2O or a dewpoint of −80°C; 4) maintaining constant flows and pressures throughout the system, and allowing time for equilibration of diffusive concentration gradients after any perturbation; 5) eliminating dead volumes; and 6) making simultaneous high-accuracy measurements of CO_2 concentrations for use in applying the dilution correction and in scientific analyses. The equipment we used to achieve these critical tasks is shown in Fig. 1 and described below.

b. Reference gases

We employed five high pressure gas cylinders to calibrate our O_2 and CO_2 measurements. These are 29.5- or 46.4-L aluminum cylinders (Luxfer) with brass Ceodeux valves, fitted with brass two-stage pressure regulators (Scott Specialty Gases, model 14). The high-span (HS), low-span (LS), and long-term (LT) reference tanks were prepared and assigned O_2 and CO_2 values in the Atmospheric Oxygen Laboratory at the Scripps Institution of Oceanography (SIO; Keeling et al. 1998a). These cylinders were also analyzed for CO_2 concentration at the National Oceanic and Atmospheric Administration (NOAA) Climate Monitoring and Diagnostics Laboratory (CMDL; Zhao et al. 1997). The HS, LS, and LT reference gases were adjusted to have nominal $\delta(O_2/N_2)$ values of −100, −600, and −300 per meg on the SIO oxygen scale and nominal CO_2 concentrations of 340, 450, and 390 ppm, respectively. Using reference gases with inverted O_2 and CO_2 ranges leads to smaller apparent mole fraction differences in the fuel-cell instrument [Eq. (3)], but more closely matches natural variations. These ranges were intended to span the full range of observations, but at low heights at night during summer they were occasionally exceeded. An additional CO_2 reference tank (CT) was prepared and assigned a CO_2 value at CMDL, with a nominal concentration of 370 ppm. The working tank (WT) reference gas was ordered (Scott–Marrin) as natural air with a nominal CO_2 concentration of 380 ppm and ambient O_2 levels, but we treat these values as unknowns in our calibration scheme.

The HS, LS, LT, and CT cylinders are connected to two miniature solenoid valve manifolds (Numatics, TM series). Miniature solenoid valves such as these can develop significant leaks, so caution and frequent automated leak checks should be applied in their use. One of these solenoid manifolds selects a reference gas or sample air to be purged, while the other selects a reference gas or sample air to be analyzed. The gas selected to be analyzed passes through a mass-flow controller (MKS Instruments, M100B) set to either 100 or 50 mL min^{-1} (see section 2c). Every 6 h the HS and LS gases are analyzed for 20 or 30 min each (see section 2d). To sweep out and condition the regulators and stagnant lines, we purge each of these gases for 15 min at 300 mL min^{-1} prior to introducing them to the analyzer. To avoid known cylinder drift near depletion (Keeling et al. 1998a, 2004, 2005; Langenfelds et al. 2005), we normally stop using the HS and LS cylinders when their pressure reaches 30 atm, and return them for reanalysis. The 46.4-L HS and LS cylinders last 6 months at a 100 mL min^{-1} measurement flow and our analysis frequency. Once every 3 days, we analyze the LT gas, after purging for 20 min at 300 mL min^{-1}, while once every 6 days we also analyze the CT gas after purging for 10 min at 300 mL min^{-1}. The 46.4-L LT and 29.5-L CT cylinders should have useful lifetimes at 100 mL min^{-1} measurement flow of 6 and 8 yr, respectively, although they should be returned to a laboratory for recalibration sooner than that. The WT gas flows to the analyzer continuously, and using 29.5-L cylinders they must be replaced every month with a 100 mL min^{-1} flow.

We determine $\delta(O_2/N_2)$ values by referencing $\Delta_{1\text{-min}}$ obtained by comparing WT and sample gases to those obtained comparing WT and other calibration gases.

We calculate the WT value and span using a linear calibration between the HS and LS values, interpolated in time between the 6-hourly calibrations. Analyses of the LT gas provide independent checks on the stability and accuracy of our O_2 calibrations. For our CO_2 measurements we use a LiCor 6251 dual-channel infrared gas analyzer (IRGA), and calculate 1-min means of the IRGA signal corresponding to the downstream switching cycle. To obtain CO_2 concentrations, we use the approximately weekly calibrations that include all four reference gases to calculate second-order polynomial calibration curves. We then apply linear adjustments to these second-order curves based on the 6-hourly HS and LS runs. For an independent check on our CO_2 measurements, we compare to the existing high-accuracy CO_2 measurement system in place at the WLEF tall tower (Bakwin et al. 1998).

c. Air sampling and drying

Another critical challenge of all atmospheric O_2 measurement systems is the delivery of air from the inlet location to the instrument without fractionating O_2 relative to N_2. For the first year of the WLEF deployment, we maintained sample flows of 100 mL min^{-1}. However, in an attempt to minimize the demands of replacing WT cylinders every month and HS and LS cylinders every 6 months, in June 2001 we reduced the flow rate to 50 mL min^{-1}. To avoid unreasonably long gas residence times in the inlet tubes at these flow rates and to take advantage of existing 10–20 L min^{-1} sample inlet lines, for three of our lines we chose to pick off a small measurement flow from the larger sample flow at a tee junction. Because tee junctions can fractionate O_2 relative to N_2, as an additional check on the effect of these tees we installed a dedicated line at 30 m with no tee (see Fig. 1). Comparisons between measurements from the 30-m lines with and without a tee then provide a means of assessing fractionation effects in the field. To further minimize pressure fluctuations at these tees, we installed 5 m of 4.3-mm ID tubing downstream of the tees and upstream of the pickoff for the Bakwin et al. (1998) CO_2 concentration system (not shown), and 15 m of 9.6-mm ID tubing downstream of the flux LiCor and upstream of the main diaphragm pumps for these lines.

As illustrated in Fig. 1, our inlets consist of a 9-cm-diameter inverted plastic funnel acting as a rain shield connected to a 5-cm-diameter, 3-μm-pore-sized filter in a plastic housing (Cole Parmer). Inside the instrument trailer, the sample air passes through 7-μm filters, then mass-flow controllers (MKS Instruments, M100B), and then to a miniature solenoid valve manifold (Numatics, TM series). For the first year and a half of the WLEF deployment, we used manual needle valves instead of mass-flow controllers on the inlet lines, but because variable pump efficiency and needle valve impedance required frequent adjustments to maintain constant flows, we switched to the illustrated configuration in February 2002. The inlet solenoid valves select one of the four inlet lines to be sampled, and direct the other three to a diaphragm pump (KNF, N010), which continuously flushes the unused lines. Gas from the selected inlet line is pressurized by a second diaphragm pump (KNF, N05) to approximately 160 kPa before entering a custom glass refrigerator trap held between 0° and 5°C. This sample pump has a Teflon valve plate and Teflon-coated neoprene diaphragm based on early success with these materials at SIO (R. Keeling 2006, personal communication). However, we must also use four Viton o-rings in custom-cut grooves in the pump heads to prevent leakage along the Teflon valve plate.

It is necessary to position the refrigerator trap lower than the pump so that any compression-induced condensation will flow downstream into the trap and not collect at the pump head. Water collected in this trap is removed by a peristaltic pump (Cole Parmer) running at 0.06 mL min^{-1}, which prevents liquid from accumulating in the trap without the potential for fractionation that would exist with an open vent (Manning 2001). The refrigerator trap removes the bulk of water vapor present in the airstream. However, because the dilution associated with only a +1 ppm change in water vapor would appear as a −1.3 per meg change in O_2, we must dry the air much further. The sample air next passes through a 2.5-cm-diameter glass trap in a cryogenic bath (FTS VT490) held below −90°C. This trap would normally last 2 weeks before clogging, but we swap it once per week with a second trap. The trap that is not in use is dried by the intake line and calibration gas purge flows (Fig. 1). After this second stage of drying, the sample gas stream joins the four calibration gases at the purge and analysis solenoid valve manifolds.

As a result of thermal diffusion, large gradients in O_2 and N_2 form going into and out of cold traps (Keeling et al. 1998a). At steady flows, conservation of mass ensures that the sample is not altered passing through the traps, but any disturbance to the pressure or flow through the traps can result in large transient responses in the instrument while these gradients reestablish. Consequently, when we are analyzing a calibration gas, we must continue to purge the traps with sample air at the same flow and pressure. The flow rate of the calibration gas purge is set by a downstream manual needle valve, while the flow rate of the sample gas is fixed by the upstream mass-flow controllers. A manual needle valve on the sample purge line then allows us to match

the trap pressures during purge and analysis. Nonetheless, even the smaller perturbations associated with switching between sample and calibration gas, or between two different sample lines, can cause noticeable transient instrument responses.

In addition to these flow perturbation effects, it is necessary to sweep out the trap volumes and unavoidable dead spaces with the new gas after switching. At our low-flow rates, this can take a considerable amount of time. We have taken care to minimize the dead volumes at pressure sensors, and within the solenoid valves and valve manifolds. In practice, it takes approximately 5 min for the CO_2 and O_2 readings to stabilize after switching between calibration gases and 10–15 min, because of the large-volume cold trap, after switching between sample lines (see Fig. 3). This sample line equilibration time could be reduced by minimizing the trap volumes further or increasing the flow rate, with the associated trade-offs being more frequent trap and reference cylinder replacement.

d. O_2 and CO_2 measurements

The reference or sample gas selected for analysis passes through the mass-flow controller mentioned above and a final cold trap, consisting of a 3-mm ID stainless steel tubing loop, before entering the CO_2 analyzer at approximately 135 kPa. The WT reference gas passes through a similar cold trap at a pressure of 160 kPa. Its pressure is then reduced through a proportional solenoid valve (MKS, 248A) driven by a feedback controller (MKS, 250E) referenced to a 10-torr full-scale differential pressure gauge (MKS, 223B), in order to match the sample and reference pressures in the CO_2 analyzer. Downstream of the CO_2 analyzer, both gas streams pass through 0.5-μm filters, mass-flow meters (Honeywell, AWM3100), and manual needle valves before reaching the four-way changeover valve described above. By adjusting these needle valves, we can balance the flows in the two lines. The four-way valve then switches once every minute to allow the rapid signal differencing and calculation of $\Delta_{1\text{-min}}$ described above. After passing through the Oxzilla sample cells, the two gas streams join in a volume connected to the internal pressure sensor before exiting to the room. Changes in room pressure, and consequently the Oxzilla cell pressure, have a significant effect on the signals from the individual Oxzilla cells. However, this effect is much smaller on the difference signal between the two cells, and virtually insignificant on the 1-min amplitude of this difference signal that we use as the basis for our measurement.

Figure 3 shows the $\Delta_{1\text{-min}}$ O_2 signal and CO_2 analyzer voltage over 24 h of routine summertime measurements, covering a full O_2 and CO_2 diurnal cycle and including four calibration periods in which gas from the HS and LS cylinders were analyzed. Using the inlet and analysis solenoid valve manifolds, we switch the gas to be analyzed every 20 or 30 min. Initially, we allowed 30

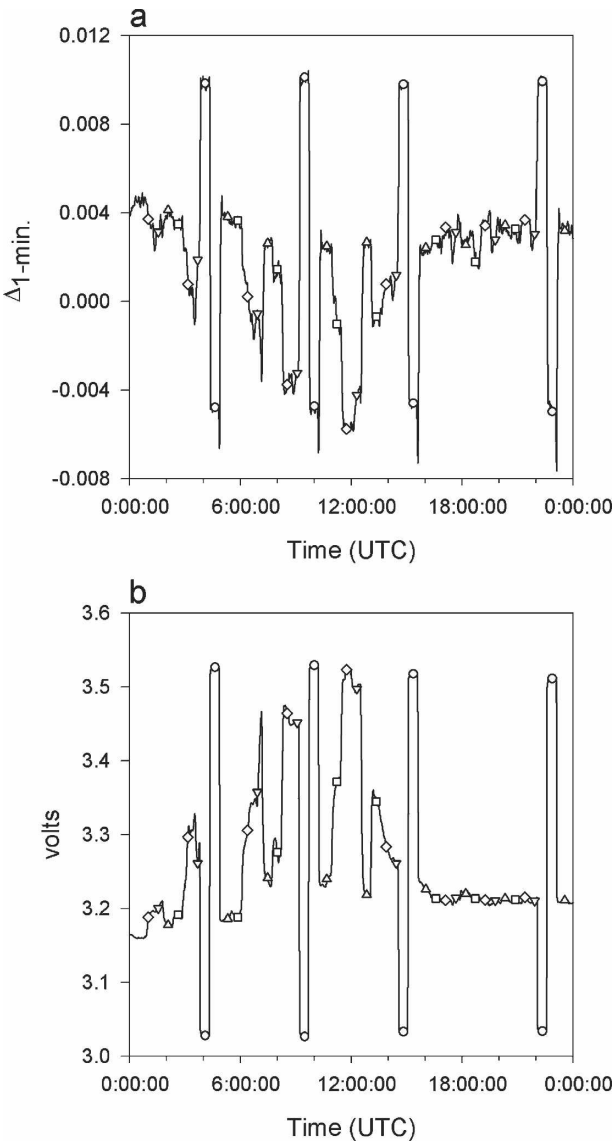

FIG. 3. Example of (a) the amplitude of the 1-min switching cycle for the Oxzilla differential O_2 signal ($\Delta_{1\text{-min}}$) and (b) the 1-min-averaged signal from the CO_2 analyzer on 9 Jun 2001. Symbols represent the averages of these values as determined from the last 6 min of each measurement period for 496 m (upward-pointing triangles), 122 m (squares), 30 m (diamonds), 30 m no tee (downward-pointing triangles), and calibration (circles) gas. Midnight (UTC) occurs at 1900 local time. The lower values of $\Delta_{1\text{-min}}$ at night correspond to less O_2 in the sample air than in the reference gas. For the CO_2 analyzer, the higher voltages at night correspond to more CO_2 in the sample air than in the reference gas.

min per line, but after installing the mass-flow controllers on each line in February 2002 we were able to reduce the switching time to 20 min. In either case, we use only the last 6 min of data from each gas for a measurement. This results in three independent $\Delta_{1\text{-min}}$ values, which average to an expected 1σ precision of 1.4 per meg. To apply the CO_2 dilution correction, a measurement accuracy of 1 ppm would be sufficient, but most scientific applications require significantly better resolution. We average the CO_2 analyzer voltage over the corresponding 6 min to achieve a 1σ precision of 0.05 ppm.

e. Potential sources of measurement bias

High-precision, comparable atmospheric O_2 measurements are still very challenging to make. Our quoted precision of ±1.4 per meg corresponds to the addition or removal of only one molecule of O_2 to every 3 million molecules of air, and there are numerous processes that can introduce biases that are 10–100 times greater in magnitude. For example, it is known that thermal fractionation of O_2 relative to N_2 inside high pressure gas cylinders resulting from small ambient temperature changes can lead to drift in $\delta(O_2/N_2)$ values for the delivered air on the order of 10–20 per meg over the life of the cylinder (Keeling et al. 1998a, 2004, 2005; Langenfelds et al. 2005). Furthermore, if the cylinders are upright and exposed to room temperature variations of several degrees Celsius, significant short-term oscillations in $\delta(O_2/N_2)$ may be produced and the potential for long-term drift may be greater (W. A. Brand 2003, personal communication).

Because of space constraints at the WLEF tall-tower site we were unable to place our reference cylinders horizontally or in an insulated enclosure. Temperature at specific points within the WLEF instrument trailer typically oscillates by 1°–2°C on a 2-h air conditioner switching cycle, and at various times when the heaters or air conditioners failed or could not meet demands, even larger diurnal temperature oscillations occurred. We see evidence of short-term variations in our reference gases in our LT record (Fig. 4), with periods of peak-to-peak variations of 10–40 per meg (approximately 2.5–10 per meg RMS) corresponding to periods of room temperature oscillations of 2°–12°C. It also appears from these records that $\delta(O_2/N_2)$ in the air delivered from the HS and LS cylinders drifted up by approximately 20 per meg during the course of their use, resulting in apparent decreases in the LT value. Interestingly, comparing pre- and postuse calibrations at SIO and the National Center for Atmospheric Research (NCAR) for the eight HS and LS cylinders used (Fig. 4, lower panel), we only saw one case of a large

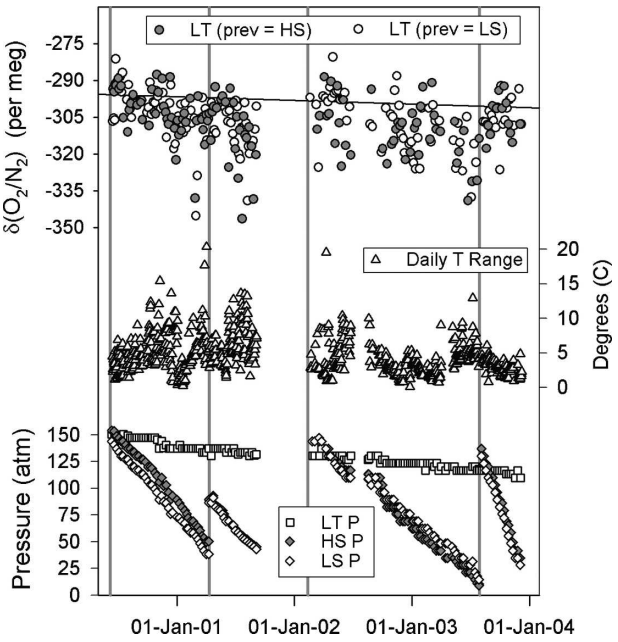

FIG. 4. (top) Determinations of the LT cylinder over 3.5 yr. The dark line connects laboratory measurements on this cylinder before and after deployment. (middle) Large short-term variations in the field LT values are associated with large room temperature variations shown here as daily room temperature ranges. (bottom) Trends in LT values appear to be related to drifts in the HS and LS reference gases as their cylinder pressures decrease. The vertical gray lines indicate times when the HS and LS gases were replaced.

change in $\delta(O_2/N_2)$. The four HS cylinders showed changes of 5, 6, 3, and −5 per meg, the four LS cylinders showed changes of 3, 1, 17, and −2 per meg, and the LT cylinder showed a change of −6 per meg. It is possible that growing concentration gradients in the vertically oriented cylinders resulted in the observed field drift in their delivered air, but that these gradients were mixed out in the process of transporting the cylinders back to the laboratory and analyzing them in a horizontal position.

Second, we know that temperature and pressure gradients at tee junctions can easily lead to $\delta(O_2/N_2)$ changes on the order of 100 per meg in the smaller flow of air going to the instrument (Manning 2001; Stephens et al. 2003). In an attempt to overcome this obstacle, we experimented with various tee configurations in which the pick-off tube extended upstream of the tee, inside of the larger inlet tube. After trying various tee sizes a pick-off tube lengths, widths, and orientations, we found that running a 1.0-mm ID, 1.6-mm OD stainless steel tube 30 cm upstream of the tee inside 9.6-mm ID tubing had less than 10 per meg fractionation at a flow ratio of approximately 200:1. We note that many other pick-off configurations led to fractionation on the order

of 100 per meg under these flow conditions. The amount of fractionation associated with a 2.1-mm ID, 3.2-mm OD pick-off tube was sensitive to the radial positioning of the tube end within the sample tube and to the orientation of the tube-end face relative to the sample flow. In contrast, the 1.0-mm ID pick-off tube that we used did not appear sensitive to these parameters. We used a high-precision vacuum ultraviolet O_2 analyzer (Stephens et al. 2003) in these tests but other limitations in the experimental design precluded tighter constraints.

Our analyses have revealed that while this tee configuration may have minimized pressure-related fractionation effects, it was still susceptible to temperature-related effects. The integration of these tees with the existing plumbing at WLEF resulted in the pick-off tubes extending upstream into tubing that was outside of the instrument trailer, black in color, and only partially shaded by existing structures. Measurements from the three lines with tees show occasional isolated O_2 anomalies, both positive and negative, on the order of 20 per meg. These anomalous measurements occur within several hours of local noon and only when it is sunny. This suggests that the pick-off tubes may have been sampling within thermally induced O_2 gradients associated with differential solar heating of the exterior tubes.

While the dedicated intake line at 30 m does provide an independent means of sampling for comparison, it is also vulnerable to potential fractionation effects, in this case resulting from thermal gradients at the inlet associated with the slower intake flows (Manning 2001; Blaine et al. 2005; Sturm et al. 2005b). The funnels we used as rain shields were white and the filter housings were light blue. For the first year of the WLEF deployment with sample flows of 100 mL min^{-1}, we did not observe clear signs of inlet fractionation. However, after reducing the flow rate to 50 mL min^{-1}, the dedicated 30-m line exhibited diurnal APO variations of up to 40 per meg in winter and up to 100 per meg in summer on sunny days with moderate winds. These variations were in the direction of low O_2 relative to N_2 during the daytime, which is consistent with sampling thermally induced gradients at the inlet associated with solar heating of the rain shield and or filter housing. Also, the magnitude of these variations is comparable to expectations from more recent inlet tests when measuring Ar/N_2 ratios (Blaine et al. 2005; Sturm et al. 2005b).

Our improved understanding of these effects will naturally lead to different procedures in future deployments. High pressure gas cylinders should be horizontal and insulated from room temperature variations to prevent short-term oscillations and long-term drift in reference values. Also, it may be possible to use pick-off tees without significant fractionation, if pressure gradients can be minimized and all tubing can be maintained isothermal for sufficient distances upstream and downstream of the tee. However, even though installation and gas residence time concerns led us to use tees on three of the lines at WLEF, we do not recommend this approach. Finally, inlet flow rates and inlet geometry should be selected to minimize the potential for stagnant air and the development of thermal gradients. The most promising inlet approach based on Ar/N_2 tests appears to be that of using a fan to aspirate the inlet (Blaine et al. 2005).

The presence of known artifacts in the WLEF O_2 data will require special care in their interpretation. For example, analyses of O_2:CO_2 ratios will need to compare cloudy and sunny days, and different times of day, to quantify potential biases in the results. Fortunately some of the strongest signals, such as the predawn vertical gradients, should be less affected by the inlet and tee fractionation effects associated with solar heating. For O_2 comparisons between WLEF and other stations, the effect of cylinder drift will have to be assessed and possibly corrected for based on pre- and postdeployment laboratory determinations of the HS and LS values, and the operational LT measurements. It is important to point out that these potential effects are not unique to the fuel-cell instrument but are general to all in situ O_2 measurement techniques. The comparability of our measurements with respect to other sites and techniques clearly depends on a number of factors. However, assuming that we can adequately filter or correct for known biases and that we can eliminate them in future deployments, we conservatively estimate comparability (see definition in Worthy and Huang 2005) with respect to other O_2 measuring programs of ± 10 per meg for our fuel-cell system. A quantitative summation of the various components contributing to this comparability limit is difficult to make, but it is the potential effects that we cannot easily detect or correct for that contribute most to our subjective estimate. These are primarily short-term fractionation in vertically oriented and uninsulated cylinders, and incomplete stabilization of concentration gradients associated with cold traps after switching between inlet lines.

We do not discuss our CO_2 measurements in detail here, but IRGAs are also known to have potential sources of bias that require careful attention to sample drying, pressure balancing, reference gas handling, and calibration schemes (Bakwin et al. 1998; Trivett and Köhler 1999). Our calibration frequency was optimized

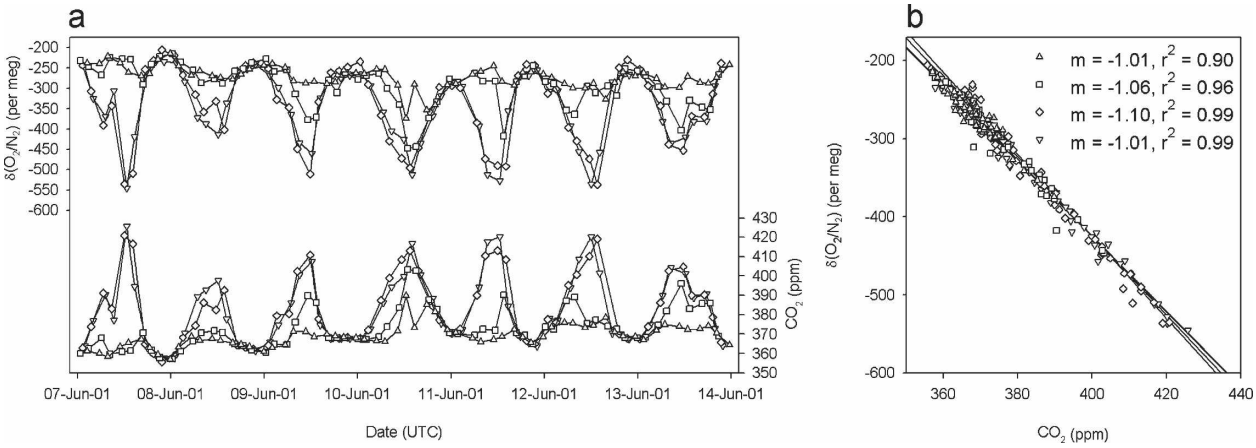

FIG. 5. Seven-day time series (a) and correlation (b) plots for atmospheric O_2 and CO_2 variations measured at the WLEF tall-tower site in June 2001 for 496 (upward-pointing triangles), 122 (squares), 30 (diamonds), and 30 m no tee (downward-pointing triangles) gases. Midnight (UTC) occurs at 1900 local time. The *y* axis in (a) and both axes in (b) have been scaled to be equivalent on a mole O_2 to mole CO_2 basis. The slopes in (b) were determined from orthogonal distance regression with uncertainties on O_2 and CO_2 values set equal on a molar basis.

for the requirements of the O_2 measurements and conservation of calibration gases, but it may not have been ideal for CO_2 measurements. The CO_2 analyzer has greater short-term drift than the O_2 analyzer because it is not calibrated by the 1-min switching cycle and has a greater thermal sensitivity. We account for short-term thermal drift in the IRGA by deriving an empirical temperature correction from our 6-hourly calibration data and apply this at the higher time resolution of the measurements. More frequent one-point calibrations or incorporating the CO_2 analyzer within the rapid switching loop would be more rigorous alternatives to this approach.

3. WLEF tall-tower observations

The WLEF tower is a 447-m-tall communications tower located in a region of mixed forest in northern Wisconsin. It is part of the NOAA/Climate Modeling and Diagnostics Laboratory (CMDL) Cooperative Sampling Network and the Department of Energy (DOE) AmeriFlux network, and is the focal point of the Chequemegon Ecosystem Atmosphere Study (ChEAS) (Bakwin et al. 1998; Davis et al. 2003; Desai et al. 2006). Ongoing measurements at the tower include CO_2 concentration at six levels; eddy covariance measurements of CO_2 flux at three levels; gas chromatography measurements of CH_4, CO, CFCs, SF_6, and N_2O concentrations at three levels; and weekly flask sampling for measurements of these and other gases. This suite of measurements has been valuable in elucidating the terrestrial ecosystem and boundary layer mixing processes affecting the atmospheric distribution of CO_2 and other species, and has encouraged the initiation of numerous collaborative studies at this site.

We deployed the O_2 system described above at the WLEF site in June 2000 and operated it semicontinuously through December 2003. Our equipment was located inside the NOAA/CMDL instrument trailer at the site. Excluding the cryogenic chiller and reference gases, the O_2 equipment fit inside a 4-ft-tall standard instrument rack. We sampled air from intake lines at three heights—396, 122, and 30 m—with a second dedicated sample line at 30 m. Figure 5 shows O_2 and CO_2 data from these four sample lines during a 1-week period in June 2001. During summer, CO_2 increases while O_2 decreases at night in response to net respiration, with the largest changes at the lowest levels. Conversely, CO_2 decreases while O_2 increases with the onset of photosynthesis and vertical mixing in the morning. The amplitude of this diurnal cycle varies with height, location, and weather, but at 30 m on a relatively calm summer day at WLEF it is typically 60 ppm in CO_2 and 300 per meg in O_2. The O_2:CO_2 relationships are strongly influenced by local photosynthesis and respiration, and the statistical errors on linear fits (Fig. 5b) to the data are very small.

During the period shown in Fig. 5, and throughout the four summers we sampled, the observed oxidation ratios ($-O_2$:CO_2) were lower than soil incubation studies would suggest (Severinghaus 1995). Caution must be applied in interpreting O_2:CO_2 slopes because it is possible for multiple processes operating at slightly different ratios, such as photosynthesis and respiration, to

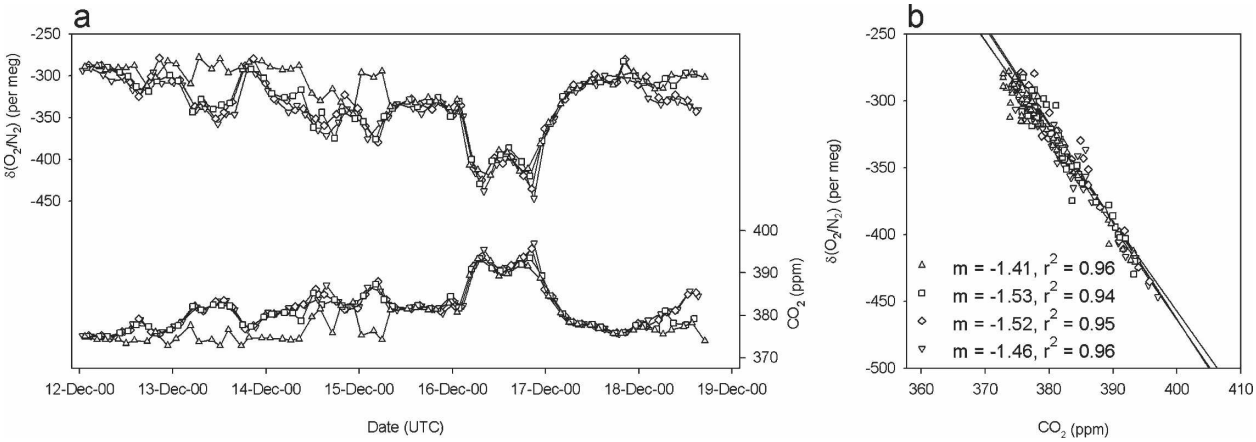

FIG. 6. Same as Fig. 5, but for a period in December 2000. The *y* axis in (a) and both axes in (b) have been expanded by a factor of 2.

result in net atmospheric changes with very different relationships than either of the individual fluxes (Seibt et al. 2004). However, when one process dominates the observed gradients, as is the case for the influence of respiration on diurnal cycles at low levels and on predawn vertical gradients, it is possible to make meaningful links between observed ratios and fluxes. For example, the low-oxidation ratios we observe in the diurnal cycles at 30 m may reflect a reliance on ammonium rather than nitrate as a nitrogen substrate for the trees, such that net oxidation of nitrogen is not occurring in the soils (Bloom et al. 1989, 1992). Finally, it is important to point out that O_2:CO_2 ratios determined from diurnal atmospheric variations cannot by themselves define the most appropriate biospheric O_2:CO_2 value to use in the global partitioning of carbon sources (Houghton et al. 2001). This value must represent the O_2:CO_2 ratio of the net change in the terrestrial carbon pool, and depends on whether this change is primarily in leaves, trunk wood, roots, soil carbon, or elsewhere. However, measurements such as these do provide valuable information on the potential variability of this value and its controlling influences.

While synoptic variations in O_2 owing to latitudinal variations in airmass origin or industrial emission signals can be detected year-round, in summer they are generally too small relative to the diurnal variations to have much influence on the observed O_2:CO_2 ratios. Figure 6 shows O_2 and CO_2 data from a week-long period in December 2000. In winter the diurnal cycle is not apparent, but the influence of synoptic pollution events can clearly be seen. During the large pollution event on 16 December, CO_2 increased by around 15 ppm and O_2 decreased by around 105 per meg. Back-trajectory analysis (not shown) indicates that this air had passed over or near both Green Bay, Wisconsin, and Chicago, Illinois. Two earlier events on 13 and 15 December, in which the lower two levels saw stronger pollution signals than the upper level, are suggestive of more local sources. Back trajectories on these days indicate westerly flows that may have been influenced by the small town of Park Falls, Wisconsin. The observed $-O_2$:CO_2 ratio (Fig. 6b) averaged over these three events of 1.46 is very close to that expected from the average mix of fossil fuel emissions in the United States in 2000 of 1.45 (Keeling 1988; Marland et al. 2005). With further work, atmospheric O_2 measurements may provide a tool for verifying fuel consumption mixtures reported for various countries or regions.

Our data also reveal a seasonal cycle with O_2 lower and CO_2 higher during winter. Because atmospheric O_2 is strongly influenced by oceanic exchange, we can compare these seasonal cycles observed at WLEF to those observed at upwind marine boundary layer sites to investigate atmospheric transport and mixing over the continents. The seasonal amplitude in atmospheric O_2 is less at WLEF than at Cold Bay, Alaska (Keeling et al. 1998b), as expected from dilution of the oceanic O_2 signal through vertical mixing over the continent. This type of comparison is particularly sensitive to any systematic biases in the O_2 measurements, but preliminary analyses suggest that our measurements will be useful in testing atmospheric transport models. Information on the vertical gradients of O_2 over the oceans and continents would of course be useful in this context, but because the seasonal O_2 cycles at marine surface sites are already relatively well predicted by coupled ocean–atmosphere models (Keeling et al. 1998b; Stephens et al. 1998) this information is not necessary for first-order tests.

4. Conclusions

We have described a new technique for making ppm-level atmospheric O_2 measurements based on the adaptation of a commercially available fuel-cell analyzer. This analyzer is well suited for unattended field-based O_2 observations because of its small size, low cost, motion insensitivity, ease of adaptation, robust operation, precision, and response time. After implementing the modifications for rapid calibrations and active pressure and flow control as described here, our analysis system achieves a precision of ±1.4 per meg for a 6-min-averaged measurement made every 20 min. This high level of performance enables a wide range of new biogeochemical investigations and monitoring efforts.

We have used the analysis system described here to measure atmospheric O_2 and CO_2 over a period of three-and-a-half years at the WLEF tall-tower research site in northern Wisconsin, and have presented several weeks of data here. The measurements define oxidative ratios for terrestrial respiration that have a bearing on plant physiology and on the application of O_2 data to constrain the global carbon cycle. By detecting the O_2:CO_2 ratios in pollution events from U.S. cities, we can calculate corresponding mixes of fuel types and explore potential methods for future emission verification. Finally, these data provide information on aspects of continental atmospheric mixing important in atmospheric transport modeling and inverse calculations.

While collecting one of the first extended records of in situ atmospheric O_2 measurements, we have encountered and characterized a number of potential sources of bias in such measurements. These include fractionation of O_2 with respect to N_2 in reference cylinders, at tubing tee junctions, and at sample inlets. The fuel-cell system has now been returned to our laboratory for refurbishment while we consider various redeployment options. In the future, we will minimize or eliminate known sources of bias by storing reference cylinders horizontally and in an insulated enclosure, by avoiding the use of tees, and by using high flow rates and air inlets designed to reduce thermal gradients. We note that our estimate of ±10 per meg comparability after screening or correcting for known biases could be improved and better quantified with these modifications, and conversely that in situ O_2 observations without careful attention to gas-handling and robust performance diagnostics may be subject to even larger measurement biases. A number of fuel-cell O_2 analyzers have recently or will soon be put into service by other investigators at continental and marine boundary layer sites around the world, ensuring significant future contributions from this approach.

Acknowledgments. We are indebted to Ralph Keeling, Bill Paplawsky, Adam Cox, and Laura Katz at the Scripps Institution of Oceanography for preparing and analyzing our reference cylinders. We thank Tara Schaefer, Frank Lenning, and staff at the Forest Sciences Laboratory in Rhinelander, Wisconsin, for assistance with field servicing and maintenance. The initial purchase of equipment and instrument deployment were supported by a Cooperative Institute for Research in the Environmental Sciences Innovative Research Program grant and later ongoing support was provided by the National Center for Atmospheric Research Atmospheric Technology Division. Reviews by Patrick Sturm and two anonymous reviewers were very helpful in improving this paper.

REFERENCES

Bakwin, P. S., P. P. Tans, D. F. Hurst, and C. Zhao, 1998: Measurements of carbon dioxide on very tall towers: Results of the NOAA/CMDL program. *Tellus,* **50B,** 401–415.

Battle, M., M. L. Bender, P. P. Tans, J. W. C. White, J. T. Ellis, T. Conway, and R. J. Francey, 2000: Global carbon sinks and their variability inferred from atmospheric O_2 and $\delta^{13}C$. *Science,* **287,** 2467–2470.

——, and Coauthors, 2006: Atmospheric potential oxygen: New observations and their implications for some atmospheric and oceanic models. *Global Biogeochem. Cycles,* **20,** GB1010, doi:10.1029/2005GB002534.

Bender, M. L., P. P. Tans, J. T. Ellis, J. Orchardo, and K. Habfast, 1994: A high precision isotope ratio mass spectrometry method for measuring the O_2/N_2 ratio of air. *Geochim. Cosmochim. Acta,* **58,** 4751–4758.

——, J. T. Ellis, P. P. Tans, R. Francey, and D. Lowe, 1996: Variability in the O_2/N_2 ratio of southern hemisphere air 1991-1994: Implications for the carbon cycle. *Global Biogeochem. Cycles,* **10,** 9–21.

Blaine, T. W., R. F. Keeling, and W. J. Paplawsky, 2005: An improved inlet for precisely measuring the atmospheric Ar/N_2 ratio. *Atmos. Chem. Phys. Discuss.,* **5,** 11 899–11 910.

Bloom, A. J., R. M. Caldwell, J. Finazzo, R. L. Warner, and J. Weissbart, 1989: Oxygen and carbon dioxide fluxes from barley shoots depend on nitrate assimilation. *Plant Physiol.,* **91,** 352–356.

——, S. S. Sukrapanna, and R. L. Warner, 1992: Root respiration associated with ammonium and nitrate absorption and assimilation by barley. *Plant Physiol.,* **99,** 1294–1301.

Davis, K. J., P. S. Bakwin, C. Yi, B. W. Berger, C. Zhao, R. M. Teclaw, and J. G. Isebrands, 2003: The annual cycles of CO_2 and H_2O exchange over a northern mixed forest as observed from a very tall tower. *Global Change Biol.,* **9,** 1278–1293.

Denning, A. S., I. Y. Fung, and D. Randall, 1995: Latitudinal gradient of atmospheric CO_2 due to seasonal exchange with land biota. *Nature,* **376,** 240–242.

Desai, A. R., and Coauthors, 2006: Influence of vegetation and surface forcing on carbon dioxide fluxes across the Upper Midwest, USA: Implications for regional scaling. *Agric. For. Meteor.,* in press.

Gurney, K. R., and Coauthors, 2002: Towards robust regional es-

timates of CO_2 sources and sinks using atmospheric transport models. *Nature,* **415,** 626–630.

Houghton, J. T., Y. Ding, D. J. Griggs, M. Noguer, P. J. van der Linden, X. Dai, K. Maskell, and C. A. Johnson, Eds., 2001: *Climate Change 2001: The Scientific Basis.* Cambridge University Press, 881 pp.

Keeling, R. F., 1988: Development of an interferometric oxygen analyzer for precise measurement of the atmospheric O_2 mole fraction. Ph.D. dissertation, Harvard University, 179 pp.

——, and S. R. Shertz, 1992: Seasonal and interannual variations in atmospheric oxygen and implications for the global carbon cycle. *Nature,* **358,** 723–727.

——, R. P. Najjar, M. L. Bender, and P. P. Tans, 1993: What atmospheric oxygen measurements can tell us about the global carbon cycle. *Global Biogeochem. Cycles,* **7,** 37–68.

——, S. C. Piper, and M. Heimann, 1996: Global and hemispheric CO_2 sinks deduced from changes in atmospheric O_2 concentration. *Nature,* **381,** 218–221.

——, A. C. Manning, E. M. McEvoy, and S. R. Shertz, 1998a: Methods for measuring changes in atmospheric O_2 concentration and their application in Southern Hemisphere air. *J. Geophys. Res.,* **103,** 3381–3397.

——, B. B. Stephens, R. G. Najjar, S. C. Doney, D. Archer, and M. Heimann, 1998b: Seasonal variations in the atmospheric O_2/N_2 ratio in relation to the kinetics of air-sea gas exchange. *Global Biogeochem. Cycles,* **12,** 141–163.

——, T. Blaine, B. Paplawsky, L. Katz, C. Atwood, and T. Brockwell, 2004: Measurement of changes in atmospheric Ar/N_2 ratio using a rapid-switching, single-capillary mass spectrometer system. *Tellus,* **56B,** 322–338.

——, A. C. Manning, B. Paplawsky, and A. Cox, 2005: On the long-term stability of O_2/N_2 reference gases. *Proc. 12th WMO/IAEA Meeting of Experts on Carbon Dioxide Concentration and Related Tracers Measurement Techniques,* WMO Tech. Doc. 1275, Toronto, ON, Canada, WMO, 131–140.

Langenfelds, R. L., M. V. van der Schoot, R. J. Francey, L. P. Steele, M. Schmidt, and H. Mukai, 2005: Modification of air standard composition by diffusive and surface processes. *J. Geophys. Res.,* **110,** D13307, doi:10.1029/2004JD005482.

Lueker, T. J., S. J. Walker, M. K. Vollmer, R. F. Keeling, C. D. Nevison, R. F. Weiss, and H. E. Garcia, 2003: Coastal upwelling air-sea fluxes revealed in atmospheric observations of O_2/N_2, CO_2 and NO. *Geophys. Res. Lett.,* **30,** 1292, doi:10.1029/2002GL016615.

Manning, A. C., 2001: Temporal variability of atmospheric oxygen from both continuous measurements and a flask sampling network: Tools for studying the global carbon cycle. Ph.D. dissertation, University of California, San Diego, 196 pp.

——, and R. F. Keeling, 2005: Global oceanic and land biotic carbon sinks from the Scripps atmospheric oxygen flask sampling network. *Tellus,* **58B,** 95–116.

——, ——, and J. P. Severinghaus, 1999: Precise atmospheric oxygen measurements with a paramagnetic oxygen analyzer. *Global Biogeochem. Cycles,* **13,** 1107–1115.

Marca, A. D., 2004: A new instrument for precise atmospheric O_2 measurements, and its use to study uptake and release of O_2 and CO_2 by terrestrial vegetation. Ph.D. dissertation, University of East Anglia, 198 pp.

Marland, G., T. A. Boden, and R. J. Andres, cited 2005: Global, regional, and national fossil fuel CO_2 emissions. *Trends: A Compendium of Data on Global Change,* Carbon Dioxide Information Analysis Center. [Available online at http://cdiac.esd.ornl.gov/trends/emis/meth_reg.htm.]

Seibt, U., W. A. Brand, M. Heimann, J. Lloyd, J. P. Severinghaus, and L. Wingate, 2004: Observations of O_2:CO_2 exchange ratios during ecosystem gas exchange. *Global Biogeochem. Cycles,* **18,** GB4024, doi:10.1029/2004GB002242.

Severinghaus, J. P., 1995: Studies of the terrestrial molecular oxygen and carbon cycles in sand dune gases and in Biosphere 2. Ph.D. dissertation, Columbia University, 148 pp.

Stephens, B. B., 1999: Field-based atmospheric oxygen measurements and the ocean carbon cycle. Ph.D. dissertation, University of California, San Diego, 221 pp.

——, R. F. Keeling, M. Heimann, K. D. Six, R. Mumane, and K. Caldeira, 1998: Testing global ocean carbon cycle models using measurements of atmospheric O_2 and CO_2 concentration. *Global Biogeochem. Cycles,* **12,** 213–230.

——, ——, and W. J. Paplawsky, 2003: Shipboard measurements of atmospheric oxygen using a vacuum-ultraviolet absorption technique. *Tellus,* **55B,** 857–878.

Sturm, P., M. Leuenberger, and M. Schmidt, 2005a: Atmospheric O_2, CO_2, and $\delta^{13}C$ observations from the remote sites Jungfraujoch, Switzerland, and Puy de Dôme, France. *Geophys. Res. Lett.,* **32,** L17811, doi:10.1029/2005GL023304.

——, ——, F. L. Valentino, B. Lehmann, and B. Ihly, 2005b: Measurements of CO_2, its stable isotopes, O_2/N_2, and ^{222}Rn at Bern, Switzerland. *Atmos. Chem. Phys. Discuss.,* **5,** 8473–8506.

Thompson, R. L., 2005: Variations in atmospheric O_2 and CO_2 in the Southern Ocean region from continuous ship-based measurements. Ph.D. dissertation, Victoria University of Wellington, 184 pp.

Tohjima, Y., 2000: Method for measuring changes in the atmospheric O_2/N_2 ratio by a gas chromatograph equipped with a thermal conductivity detector. *J. Geophys. Res.,* **105,** 14 575–14 584.

——, H. Mukai, T. Machida, Y. Nojiri, and M. Gloor, 2005: First measurements of the latitudinal atmospheric O_2 and CO_2 distribution across the Western Pacific. *Geophys. Res. Lett.,* **32,** L17805, doi:10.1029/2005GL023311.

Trivett, N., and A. Köhler, 1999: Guide on sampling and analysis techniques for chemical constituents and physical properties in air and precipitation as applied at stations of the Global Atmosphere Watch. Part 1: Carbon dioxide. WMO Tech. Doc. 980, 63 pp.

Worthy, D., and L. Huang, 2005: 12th WMO/IAEA Meeting of Experts on Carbon Dioxide Concentrations and Related Tracers Measurement Techniques. WMO Tech. Doc. 1275, Toronto, ON, Canada, WMO, 264 pp.

Zhao, C. L., P. P. Tans, and K. W. Thoning, 1997: A high precision manometric system for absolute calibrations of CO_2 in dry air. *J. Geophys. Res.,* **102,** 5885–5894.